

1973

Hall mobility and magnetoresistance of n-type magnesium germanide

Puo-wen Li
Iowa State University

Follow this and additional works at: <https://lib.dr.iastate.edu/rtd>

 Part of the [Condensed Matter Physics Commons](#)

Recommended Citation

Li, Puo-wen, "Hall mobility and magnetoresistance of n-type magnesium germanide " (1973). *Retrospective Theses and Dissertations*. 6156.
<https://lib.dr.iastate.edu/rtd/6156>

This Dissertation is brought to you for free and open access by the Iowa State University Capstones, Theses and Dissertations at Iowa State University Digital Repository. It has been accepted for inclusion in Retrospective Theses and Dissertations by an authorized administrator of Iowa State University Digital Repository. For more information, please contact digirep@iastate.edu.

INFORMATION TO USERS

This dissertation was produced from a microfilm copy of the original document. While the most advanced technological means to photograph and reproduce this document have been used, the quality is heavily dependent upon the quality of the original submitted.

The following explanation of techniques is provided to help you understand markings or patterns which may appear on this reproduction.

1. The sign or "target" for pages apparently lacking from the document photographed is "Missing Page(s)". If it was possible to obtain the missing page(s) or section, they are spliced into the film along with adjacent pages. This may have necessitated cutting thru an image and duplicating adjacent pages to insure you complete continuity.
2. When an image on the film is obliterated with a large round black mark, it is an indication that the photographer suspected that the copy may have moved during exposure and thus cause a blurred image. You will find a good image of the page in the adjacent frame.
3. When a map, drawing or chart, etc., was part of the material being photographed the photographer followed a definite method in "sectioning" the material. It is customary to begin photoing at the upper left hand corner of a large sheet and to continue photoing from left to right in equal sections with a small overlap. If necessary, sectioning is continued again — beginning below the first row and continuing on until complete.
4. The majority of users indicate that the textual content is of greatest value, however, a somewhat higher quality reproduction could be made from "photographs" if essential to the understanding of the dissertation. Silver prints of "photographs" may be ordered at additional charge by writing the Order Department, giving the catalog number, title, author and specific pages you wish reproduced.

University Microfilms

300 North Zeeb Road
Ann Arbor, Michigan 48106

A Xerox Education Company

73-16,963

LI, Puo-wen, 1942-
HALL MOBILITY AND MAGNETORESISTANCE OF
N-TYPE MAGNESIUM GERMANIDE.

Iowa State University, Ph.D., 1973
Physics, solid state

University Microfilms, A XEROX Company, Ann Arbor, Michigan

**Hall mobility and magnetoresistance of
n-type magnesium germanide**

by

Puo-wen Li

**A Dissertation Submitted to the
Graduate Faculty in Partial Fulfillment of
The Requirements for the Degree of
DOCTOR OF PHILOSOPHY**

Department: Physics

Major: Solid State Physics

Approved:

Signature was redacted for privacy.

In Charge of Major Work

Signature was redacted for privacy.

For the Major Department

Signature was redacted for privacy.

For the Graduate College

Iowa State University

Ames, Iowa

1973

PLEASE NOTE:

Some pages may have
indistinct print.

Filmed as received.

University Microfilms, A Xerox Education Company

TABLE OF CONTENTS

	Page
ABSTRACT	vi
I. INTRODUCTION	1
II. SAMPLE PREPARATION	3
III. EXPERIMENTAL METHOD	7
IV. ELECTRICAL RESISTIVITY	8
A. Intermediate Concentration Region	8
B. High Concentration Region	13
V. HALL COEFFICIENT	14
VI. HALL MOBILITY	18
A. Acoustic Mode Scattering	21
B. Ionized Impurity Scattering	22
C. Neutral Impurity Scattering	26
D. Space Charge Scattering	27
VII. MAGNETORESISTANCE	30
A. Theoretical Considerations	30
B. Results and Analysis	35
VIII. CONCLUSIONS	50
IX. LITERATURE CITED	52
X. ACKNOWLEDGMENTS	55
XI. APPENDIX	56

LIST OF TABLES

	Page
Table 1. Values of activation energies ϵ_1 and ϵ_2 , exhaustion Hall coefficient $(R_H)_{\text{exh}}$, exhaustion carrier concentration n_0 , the estimated number of donors N_D , the mean interdonor distance r_s , the ratio r_s to the effective Bohr radius a_0 , and the mobility ratio b for seven n-type Mg_2Ge samples.	11
Table 2. Magnetoresistance coefficients in terms of the Hall mobility, anisotropy parameter, and relaxation time for $\langle 100 \rangle$ type constant energy spheroids.	33
Table 3. Magnetoresistance coefficients b , c , and d , the dimensionless Seitz coefficients b' , c' , and d' , the anisotropy parameter K , and the scattering factor $\langle \tau \rangle \langle \tau^3 \rangle / \langle \tau^2 \rangle^2$ of n-type Mg_2Ge .	43
Table 4. Analysis of Mg, used in the preparation of Mg_2Ge , for impurities.	59
Table 5. Analysis of Mg_2Ge samples for impurities.	60

LIST OF FIGURES

	Page
Fig. 1. Crystal orientation for obtaining all three magneto-resistance coefficients from a single sample of Mg_2Ge . The current \vec{I} is in the $[112]$ direction and the magnetic field \vec{H} is allowed to vary in the $(\bar{1}10)$ plane.	5
Fig. 2. Temperature dependence of the resistivity of Mg_2Ge from 4.2 K to 300 K. The intrinsic line was obtained from Redin <i>et al.</i> The resistivities of samples 1-5 can be described by Eq. (1). The resistivities of the heavily doped samples 6 and 7 are almost independent of temperature below 30 K as expected for a degenerate electron gas.	10
Fig. 3. Temperature dependence of the Hall coefficient of Mg_2Ge from 4.2 K to 300 K. The intrinsic line was obtained from Redin <i>et al.</i> The Hall coefficients of samples 1-5 all have conspicuous maxima due to impurity band conduction. The Hall coefficients of the heavily doped samples 6 and 7 are almost independent of temperature and suggest overlapping of the conduction band and impurity band.	16
Fig. 4. Temperature dependence of the Hall mobility of Mg_2Ge from 4.2 K to 300 K. Sample 2 showed marked inhomogeneity in resistivity at 77 K, the other samples were quite homogeneous. For the homogeneous samples the Hall mobility from 150 K to 300 K had a $T^{-3/2}$ temperature dependence, which indicates that intravalley acoustic mode scattering is dominant in this temperature range and that the symmetry of the conduction band minima is X_3 rather than X_1 .	20
Fig. 5. The anomalous temperature dependence of the Hall mobility of sample 2, which was found to be homogeneous in resistivity at 300 K but inhomogeneous at 77 K. For temperatures greater than 300 K the mobility is limited only by acoustic mode scattering. For temperatures less than 200 K the mobility is limited by a combination of acoustic mode scattering and space charge scattering. The anomalous hump in the mobility curve between 200 K and 300 K occurs in the transition region.	25

- Fig. 6. The longitudinal and transverse magnetoresistance $\Delta\rho/\rho_0$ of seven samples of Mg_2Ge , which show the normal H^2 magnetic field dependence for H up to 8 kOe. The symbol L represents longitudinal ($\vec{I} \parallel \vec{H}$) and the symbol T represents transverse ($\vec{I} \perp \vec{H}$) magnetoresistance. 37
- Fig. 7. The magnetoresistance effect in Mg_2Ge showing the angular dependence of $\Delta\rho/\rho_0 H^2$ at 77 K. For each sample $\Delta\rho/\rho_0 H^2$ is described by Eq. (16), and a set of magnetoresistance coefficients b , c , and d can be obtained from each curve. Since $b + c + d = 0$ and $d < 0$ we conclude that n-type Mg_2Ge is a many-valley semiconductor with constant energy spheroids in the $\langle 100 \rangle$ directions. 39
- Fig. 8. The magnetoresistance effect in Mg_2Ge showing the angular dependence of $\Delta\rho/\rho_0 H^2$ for sample 4 at four stable temperatures. The symmetry condition for $\langle 100 \rangle$ type spheroids is satisfied at all four temperatures. The values of the anisotropy parameter K were found to decrease from 2.13 at 299.5 K to 1.65 at 43.6 K. 41
- Fig. 9. The magnetoresistance effect of Mg_2Ge showing the angular dependence of $\Delta\rho/\rho_0 H^2$ at 77 K for three inhomogeneous samples. Values of $\Delta\rho/\rho_0 H^2$ are about an order of magnitude higher than the values for homogeneous samples shown in Fig. 7. $\Delta\rho/\rho_0 H^2$ was insensitive to the angle θ between \vec{I} and \vec{H} in sharp contrast to the effects observed with homogeneous samples (Figs. 7 and 8). 48
- Fig. 10. Block diagram of the apparatus. 58

ABSTRACT

The electrical resistivity, Hall coefficient, and weak-field magnetoresistance of homogeneous single crystals of n-type Mg_2Ge have been measured. The samples were either Al-doped or undoped, and had exhaustion carrier concentrations from $1.3 \times 10^{16} \text{ cm}^{-3}$ to $8.2 \times 10^{17} \text{ cm}^{-3}$. The electrical resistivity and Hall coefficient were measured from 4.2 K to 300 K. Impurity band conduction was observed at the lower temperatures. The Hall mobility from 150 K to 300 K had a $T^{-3/2}$ temperature dependence which indicates that intravalley acoustic mode scattering is the dominant scattering mechanism in this temperature range. From a consideration of the selection rules and this Hall mobility temperature dependence, we conclude that the symmetry of the conduction band minima is X_3 rather than X_1 . The weak-field magnetoresistance of Mg_2Ge , which was measured at 77.4 K and at three other stable temperatures (43.6 K, 194.5 K and 299.5 K), was found to be much smaller than the magnetoresistance of Ge and Mg_2Sn . The magnetoresistance coefficients b, c, and d were obtained from these measurements and found to satisfy the symmetry relations $b + c + d = 0$, $d < 0$. This result confirms the theoretical prediction that n-type Mg_2Ge is a many-valley semiconductor with constant energy spheroids in the $\langle 100 \rangle$ directions. The anisotropy parameter K was between 1.51 and 1.78 at 77 K. Inhomogeneous samples showed anomalies in the Hall mobilities and in the magnetoresistances.

I. INTRODUCTION

Magnesium germanide is a semiconductor of the Mg_2X family (where X can be Si, Ge, Sn, or Pb) which crystallizes in the antiferroite structure. The space group for Mg_2Ge is $Fm\bar{3}m$. A fairly complete study of the Hall mobility of Mg_2Ge above 77 K has been made by Redin *et al.*¹ However, no work has been reported on the Hall mobility of Mg_2Ge below 77 K. The first objective of this work was to study the electrical properties of n-type Mg_2Ge from 4.2 K to 77 K.

The electronic structure of the Mg_2X compounds has been investigated theoretically by Lee,² Folland,³ Folland and Bassani,⁴ Au-Yang and Cohen,⁵ and Van Dyke and Herman.⁶ Three of these theoretical papers^{2,4,5} predict that Mg_2Ge has its valence band maximum at the center of the Brillouin zone Γ , with symmetry Γ_{15} , and has its conduction band minima at the points X which are in the $\langle 100 \rangle$ directions. Experimentally, the piezoresistance measurements on n-type Mg_2Si by Whitten and Danielson⁷ and on n-type Mg_2Sn by Crossman and Danielson,⁸ and the magnetoresistance study of Mg_2Sn by Umeda⁹ have shown the conduction band of these two semiconductors to be many-valleyed with minima in the $\langle 100 \rangle$ directions. Magnetoresistance measurements of Mg_2Pb by Stringer and Higgins¹⁰ have shown that this compound also obeys the symmetry conditions for $\langle 100 \rangle$ type spheroids. Stella *et al.*¹¹ have reported the pressure coefficients of the band gaps of Mg_2Si and Mg_2Ge to be nearly the same which suggests that the symmetries of the band gaps for these two compounds may be similar. Infrared absorption experiments by Lott and Lynch¹² indicate that the band

gap of Mg_2Ge is indirect and has a valence band maximum at Γ . However, no direct experimental work has been reported on the orientation of the conduction band minima of Mg_2Ge . The band calculation by Lee² suggested that the conduction band minima of Mg_2Ge have X_1 symmetry, but more recent work by Au-Yang and Cohen⁵ showed that the conduction band minima have X_3 symmetry. Folland and Bassani⁴ examined the selection rules of Mg_2Ge and indicated that the Hall mobility temperature dependence near room temperature can be used to identify this symmetry. The second objective of this research was to determine the orientation of the conduction band minima of Mg_2Ge experimentally by the measurement of magnetoresistance, and to determine the symmetry of the conduction band minima from the Hall mobility temperature dependence near room temperature.

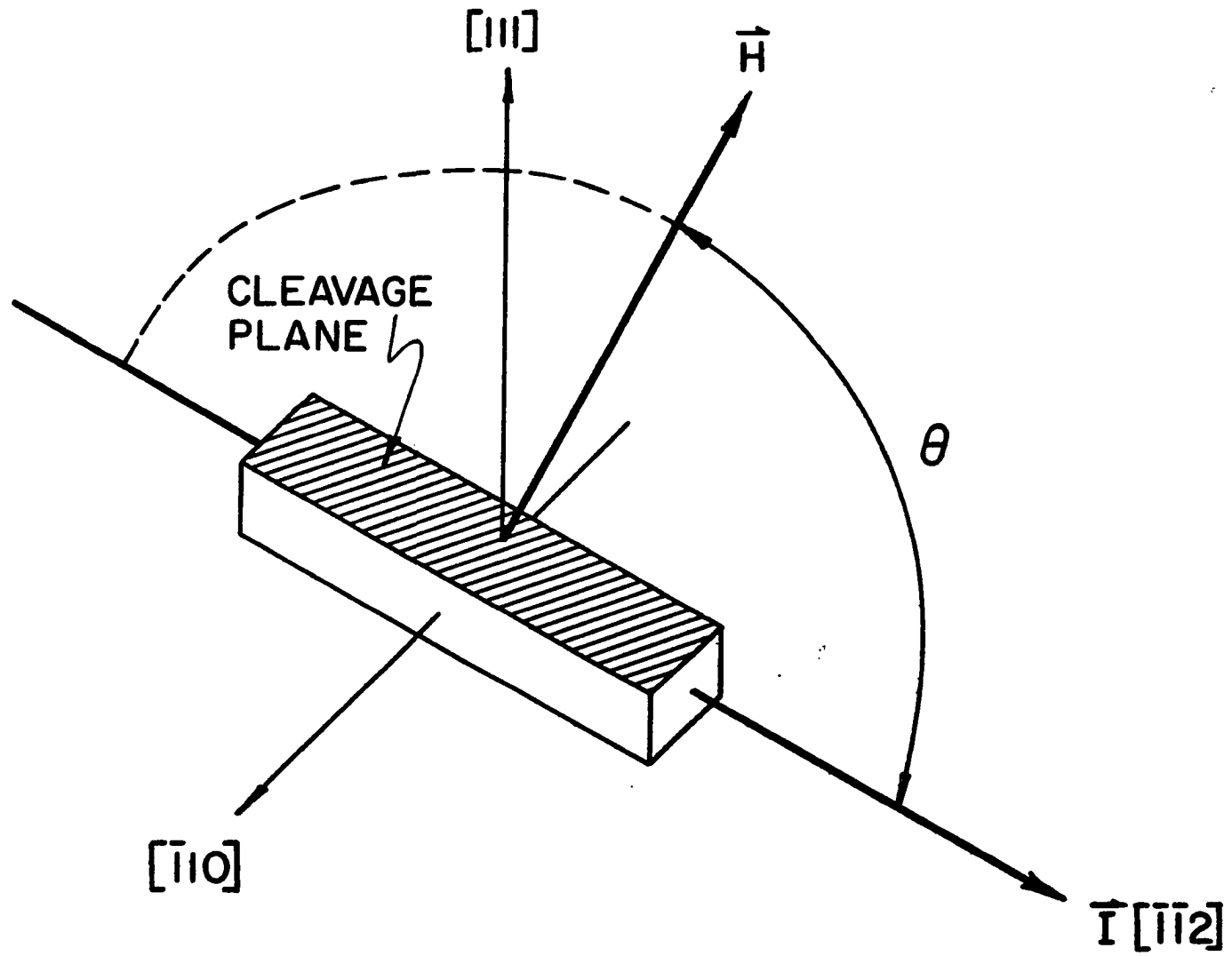
II. SAMPLE PREPARATION

Single crystals of Mg_2Ge were prepared by a modified Bridgman method in which the molten compound with a temperature gradient of 25 K per cm was cooled through the freezing point (1388 K). Single crystals 2 cm in diameter and 6 cm long were frequently obtained.

In order to produce a pure compound semiconductor it is desirable to have pure constituents. High purity germanium was available from commercial sources, but commercially available magnesium was rather impure. The stated purity of Dow Chemical Company magnesium was 99.95 percent. It was therefore necessary to develop a method for purification of the magnesium. The method developed by Grotzky and Sidles¹³ was found to be successful. The magnesium was placed in a vacuum furnace and purified by sublimation at a pressure of 10^{-9} Torr. The starting magnesium had a resistivity ratio $\rho_{300 K}/\rho_{4.2 K}$ of 200 to 400; the purified material had a resistivity ratio of about 2000. Mass spectrographic analysis at the Ames Laboratory showed a substantial reduction in the total amount of impurities.¹⁴ The mass spectrographic analysis of Mg for impurities is shown in the Appendix (Table 4).

Instead of the more conventional $[110]$ oriented crystal¹⁵ in order to obtain all three magnetoresistance coefficients b , c , and d from a single sample, we used the orientation shown in Fig. 1. The current \vec{I} is along the direction $[\bar{1}\bar{1}2]$ which lies in the cleavage plane. The direction of the magnetic field is allowed to vary in the $(\bar{1}10)$ plane which contains the directions $[111]$ and $[\bar{1}\bar{1}2]$. It is easy

Fig. 1. Crystal orientation for obtaining all three magnetoresistance coefficients from a single sample of Mg_2Ge . The current \vec{T} is in the $[\bar{1}\bar{1}2]$ direction and the magnetic field \vec{H} is allowed to vary in the $(\bar{1}10)$ plane.



to prepare such samples with accurate orientations, since Mg_2Ge single crystals cleave along the (111) plane very easily. The resistivity and Hall coefficient were also measured as functions of temperature for the same sample.

Samples were roughly oriented from observation of the (111) cleavage planes, and accurately oriented within two degrees of the required orientation by x-ray diffraction. The oriented samples were cut from the ingot by a wire saw, lapped by hand, and cleaned by an air abrasive. Dimensions of the samples were $1.4 \times 1.4 \times 12 \text{ mm}^3$. Samples exposed to air for 24 hours showed little deterioration. In the presence of water vapor Mg_2Ge will deteriorate, probably forming GeH_4 and MgO . The samples were tested for electrical homogeneity by moving resistivity probes along the sample first at room temperature and then at liquid nitrogen temperature. Both homogeneous and inhomogeneous samples were used in this experiment in order to identify spurious effects.

III. EXPERIMENTAL METHOD

A description of the apparatus used for this experiment has been given by Lee.¹⁶ Briefly, all resistivities and Hall coefficients were measured by a Rubicon potentiometer with a Keithley 148 nanovoltmeter as a null detector. A Keithley 640 vibrating capacitor electrometer was required when the resistance of the sample was very high. For magnetoresistance measurements a highly stable constant current of 1 to 30 mA was obtained from a constant current supply designed by Kroeger and Rhinehart¹⁷ at the Ames Laboratory. The change in voltage due to the magnetic field was read within 50 nV from a Rubicon model 2772 potentiometer. The magnetoresistance data were measured at 15° intervals from zero to 180°. Four readings were taken at each angle corresponding to both directions of the magnetic field and of the current. Spurious voltages, such as those arising from Hall and thermal effects, were thereby minimized.

A block diagram of the experimental arrangement is shown in the Appendix (Fig. 10).

IV. ELECTRICAL RESISTIVITY

The resistivities versus reciprocal temperature of seven n-type Mg₂Ge samples from 4.2 K to 300 K are shown in Fig. 2. Only sample 2 shows intrinsic behaviour within our temperature range. The intrinsic line for sample 2 agreed well with the extension of the intrinsic line obtained by Redin et al.¹

A. Intermediate Concentration Region

The temperature dependence of the resistivity ρ_0 for samples 1-5 may be represented by the sum of three exponentials as suggested by Fritzsche¹⁸

$$1/\rho_0 = C_1 \exp(-\epsilon_1/kT) + C_2 \exp(-\epsilon_2/kT) + C_3 \exp(-\epsilon_3/kT), \quad (1)$$

where ϵ_1 , ϵ_2 , and ϵ_3 represent activation energies. The quantity ϵ_1 is the activation energy for exciting an electron into the conduction band, and ϵ_3 is the activation energy for impurity conduction. In the theoretical model impurity conduction occurs by electrons hopping from occupied to unoccupied donor states with the aid of phonons.^{19,20} The quantity ϵ_2 is the activation energy for thermal excitation of electrons from the donor ground state to an impurity band formed by the interaction of ionized donors.^{21,22} The resulting ϵ_1 and ϵ_3 values of these five samples are shown in Table 1. The temperature region represented by ϵ_2 for these samples does not have a distinct linear range as reported by Fritzsche¹⁸ for germanium. Rather this

Fig. 2. Temperature dependence of the resistivity of Mg_2Ge from 4.2 K to 300 K. The intrinsic line was obtained from Redin et al. The resistivities of samples 1-5 can be described by Eq. (1). The resistivities of the heavily doped samples 6 and 7 are almost independent of temperature below 30 K as expected for a degenerate electron gas.

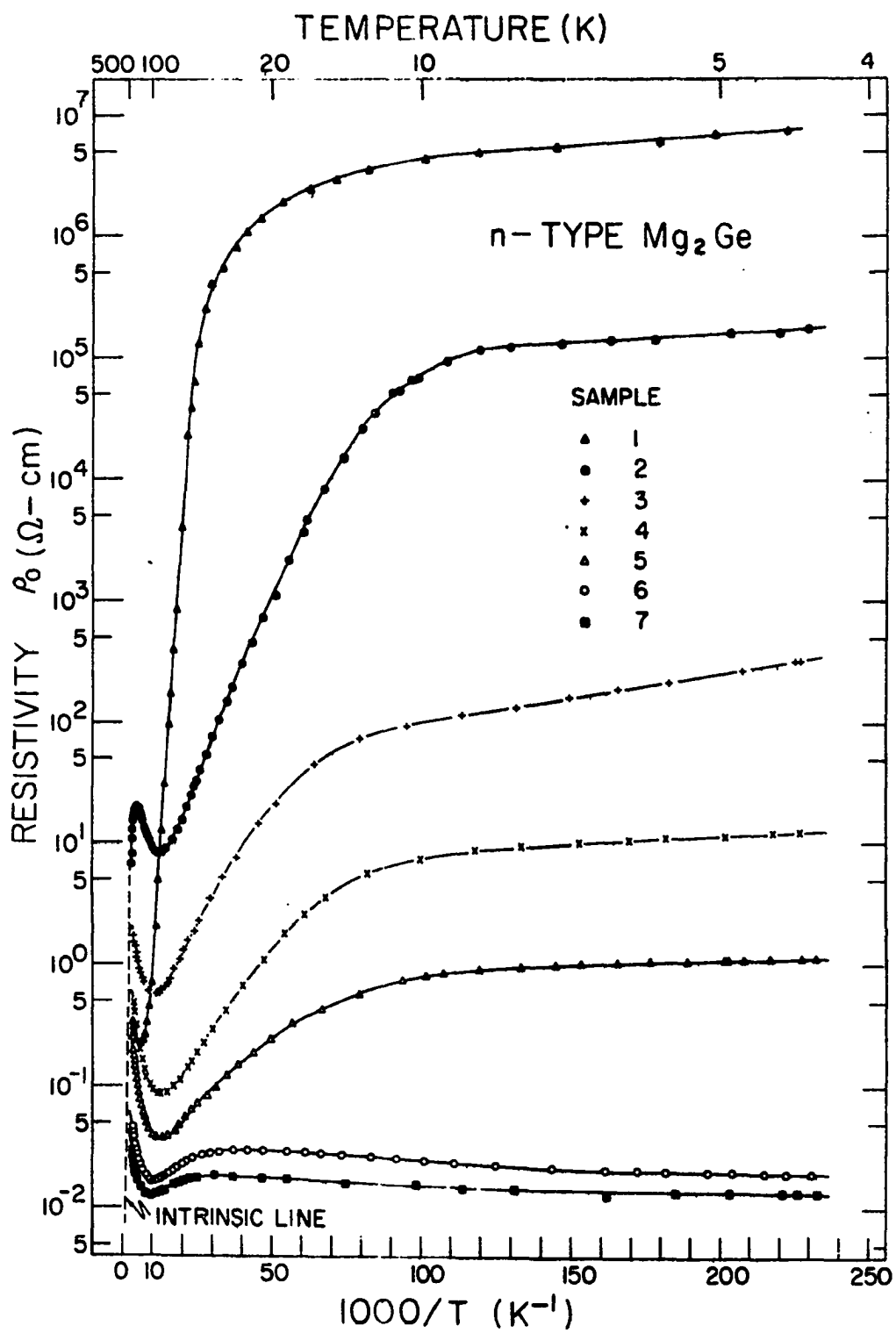


Table 1. Values of activation energies ϵ_1 and ϵ_3 , exhaustion Hall coefficient $(R_H)_{\text{exh}}$, exhaustion carrier concentration n_0 , the estimated number of donors N_D , the mean interdonor distance r_s , the ratio of r_s to the effective Bohr radius a_0 , and the mobility ratio b for seven n-type Mg_2Ge samples.

Sample	Doping Agent (at.ppm)	ϵ_1 (10^{-3}eV)	ϵ_3 (10^{-4}eV)	$-(R_H)_{\text{exh}}$ ($10\text{ cm}^3/\text{C}$)	$n_0=(N_D-N_A)$ (10^{16} cm^{-3})	N_D (10^{16} cm^{-3})	r_s (\AA)	r_s/a_0 ($a_0=31.2\text{\AA}$)	$b=\mu_c/\mu_i$
1	None	73.1	3.43	9.30	6.71	8.41	142	4.55	7.7×10^6
2	None	12.8	2.87	520	0.12	1.42	256	8.21	1.5×10^3
3	None	7.33	8.06	46.5	1.34	6.29	156	5.00	40
4	Al (82)	7.23	2.21	14.8	4.22	5.67	162	5.19	39
5	Al (82)	4.70	1.32	6.27	9.96	> 9.96	< 134	< 4.29	17
6	Al (152)	^a	^a	1.35	46.2	> 46.2	< 80.2	< 2.57	3.3
7	Al (154)	^a	^a	0.76	82.1	> 82.1	< 66.2	< 2.12	2.9

^aMetallic conduction.

region is characterized by a gradual change in slope between the temperature regions represented by ϵ_1 and ϵ_3 .

In order to compare the thermal ionization energy E_D with the experimental ϵ_1 values, we assume a hydrogenic nature for the donor impurities and estimate the thermal ionization energy from the expression²³ $E_D(\text{eV}) = (13.6/\epsilon_0^2)(m^*/m_0)$, where m_0 is the free electron mass. According to McWilliams and Lynch,²⁴ the static dielectric constant ϵ_0 of Mg_2Si is 20, and we assume the static dielectric constant of Mg_2Ge is also about 20. The electron effective mass m^* of Mg_2Ge according to Redin et al.¹ was estimated to be about $0.18 m_0$. These two values give $E_D = 6.12 \times 10^{-3}$ eV which is only half the value $\epsilon_1 = 1.28 \times 10^{-2}$ eV of sample 2.

Lee² obtained theoretical electron effective masses of $m_l^* = 0.63 m_0$ and $m_t^* = 0.25 m_0$. If we assume m^* is approximately the geometric mean mass,²³ obtained from the expression $m^* = (m_l^* m_t^{*2})^{1/3}$, then $m^* \approx 0.34 m_0$. The m^* value gives $E_D = 1.16 \times 10^{-2}$ which is in good agreement with the experimental ϵ_1 value of sample 2. We believe, therefore, that the mean effective mass for the electrons in Mg_2Ge is closer to $0.34 m_0$ calculated by Lee² than to $0.18 m_0$ estimated by Redin et al.¹

The decrease in ϵ_1 for sample 3, 4, and 5, when compared to sample 2, is due to the increased broadening of the impurity band.²⁵ The value of ϵ_1 for sample 1 is seven times greater than the estimated value of E_D . Therefore, this deep lying donor level can not be understood on the basis of the simple hydrogen model. This large value of ϵ_1 was also obtained for two additional samples. Its nature is unknown.

B. High Concentration Region

The almost temperature independent resistivities of sample 6 and 7 below 30 K is characteristic of a degenerate electron gas. The transition to metallic conduction has been predicted by Mott and Twose²⁰ to occur when the ratio of the mean interdonor distance r_s to the effective Bohr radius a_0 is about 3; that is,

$$r_s/a_0 \approx 3. \quad (2)$$

Here $r_s = (3/4 \pi N_D)^{1/3}$, where N_D is the donor concentration; and $a_0 = \epsilon_0 (m_0/m^*) a_H$ where a_H (0.53 \AA) is the Bohr radius of a hydrogen atom.

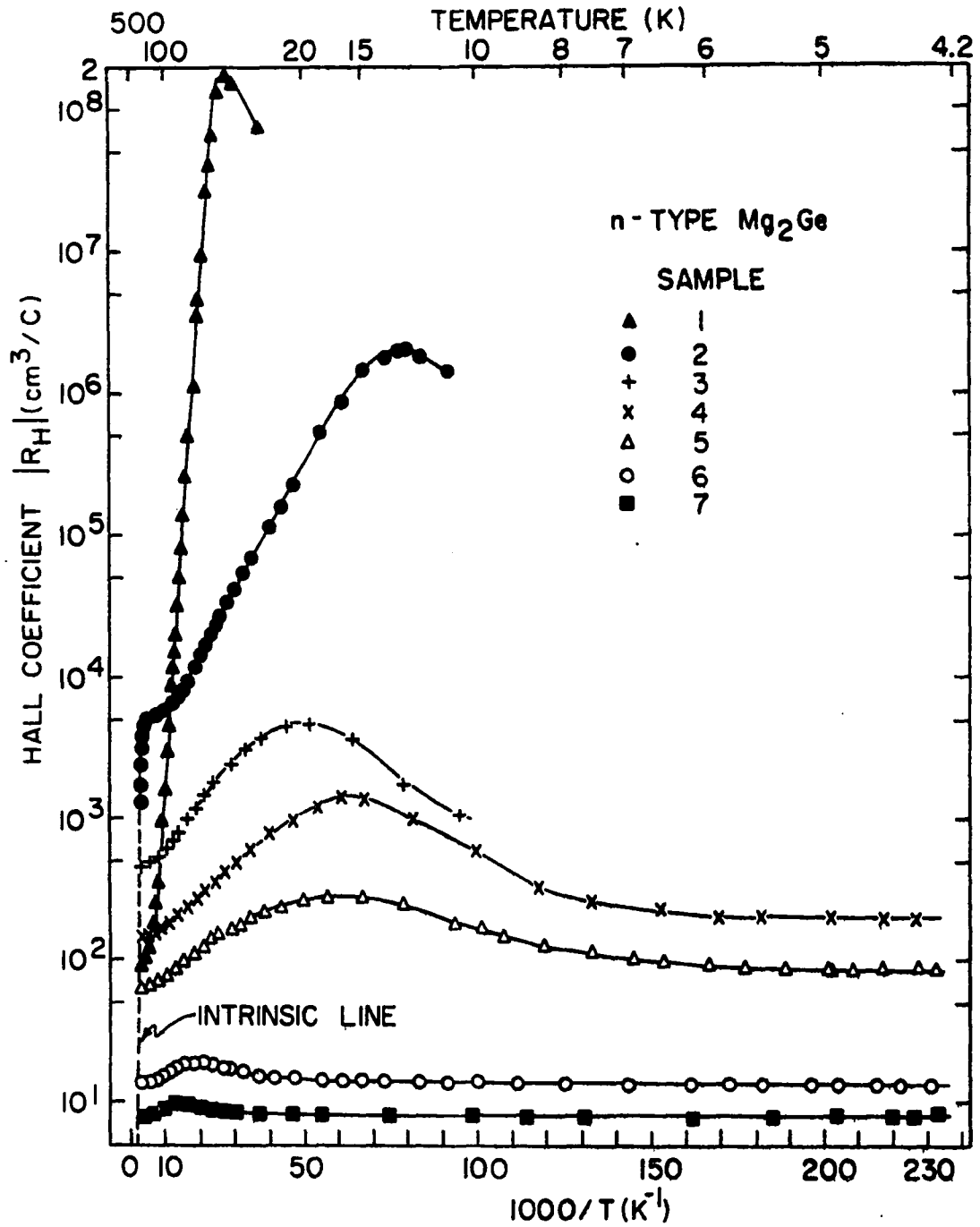
Table 1 shows the mean interdonor distance r_s for each sample. If we take Lee's mean effective mass $m^* = 0.34 m_0$ and $\epsilon_0 = 20$, we obtain an effective Bohr radius $a_0 = 31.2 \text{ \AA}$. Equation (2) is then satisfied for the highly doped samples 6 and 7 only. This result is consistent with the flat resistivity curves of samples 6 and 7 shown in Fig. 2.

V. HALL COEFFICIENT

The Hall coefficients R_H versus reciprocal temperature are shown in Fig. 3 for samples 1-7 in the temperature range 4.2 K to 300 K. Hall coefficients were measured nearly down to 4.2 K for samples 4-7. However, the Hall voltage was difficult to measure below 10 K for samples 2 and 3 and below 27 K for sample 1 because of contact noise and small Hall signals. The Hall coefficient in the intrinsic range of sample 2 agrees with the intrinsic line by Redin et al.¹ The Hall coefficients of all samples remained negative throughout the entire temperature range indicating donor impurities in the extrinsic range, and electron mobilities greater than hole mobilities in the intrinsic range. R_H was independent of magnetic field strength at least up to 8 kOe. The formula $R_H = -1/(N_D - N_A)e$ was used to obtain the exhaustion carrier concentration $n_0 = (N_D - N_A)$ shown in Table 1. For simplicity we neglect the factor $3\pi/8$ and assume the Hall mobility and drift mobility to be equal.

The Hall coefficient curves in Fig. 3 of samples 1-7 all have conspicuous maxima. Hung and Gliessman,²⁶ and Conwell²⁷ interpreted the Hall coefficient for a sample with an intermediate or high concentration of donor impurities in terms of a two-band model - a conduction band and an impurity band. We have used this two-band model to analyze the Hall data for samples 1-7. The carrier concentration and mobility are represented by n_c and μ_c in the conduction band and by n_i and μ_i in the impurity band. Introducing the mobility ratio $b = \mu_c/\mu_i$ and assuming this ratio is temperature independent, Conwell²⁷ gives an

Fig. 3. Temperature dependence of the Hall coefficient of Mg_2Ge from 4.2 K to 300 K. The intrinsic line was obtained from Redin et al. The Hall coefficients of samples 1-5 all have conspicuous maxima due to impurity band conduction. The Hall coefficients of the heavily doped samples 6 and 7 are almost independent of temperature and suggest overlapping of the conduction band and impurity band.



expression for b in terms of the exhaustion Hall coefficient $(R_H)_{\text{exh}}$ and the maximum Hall coefficient $(R_H)_{\text{max}}$

$$(R_H)_{\text{exh}} / (R_H)_{\text{max}} = 4b / (b + 1)^2. \quad (3)$$

The values of $(R_H)_{\text{max}}$ may be obtained from Fig. 3, and the values of $(R_H)_{\text{exh}}$ are given in Table 1. The b values calculated from Eq. (3) for samples 1-7 are also shown in Table. 1.

VI. HALL MOBILITY

The Hall mobilities $\mu_H = R_H/\rho_0$ for samples 1-7 are shown as functions of temperature in Fig. 4. Samples 6 and 7, which have the highest impurity content, have electron mobilities which are nearly temperature independent below 40 K. Such behavior is characteristic of a degenerate electron gas. At temperatures below 10 K the mobilities of the electrons for samples 6 and 7 are much greater than for the other samples. Similar crossing of the mobility curves has been reported by Conwell²⁷ on Ge and on GaP by Casey *et al.*²⁸

At very low temperatures, samples 1-5 have electron mobilities which decrease sharply with decreasing temperature owing to the onset of impurity band conduction. The expression for mobility in the two-band model, according to Khosla,²⁹ is

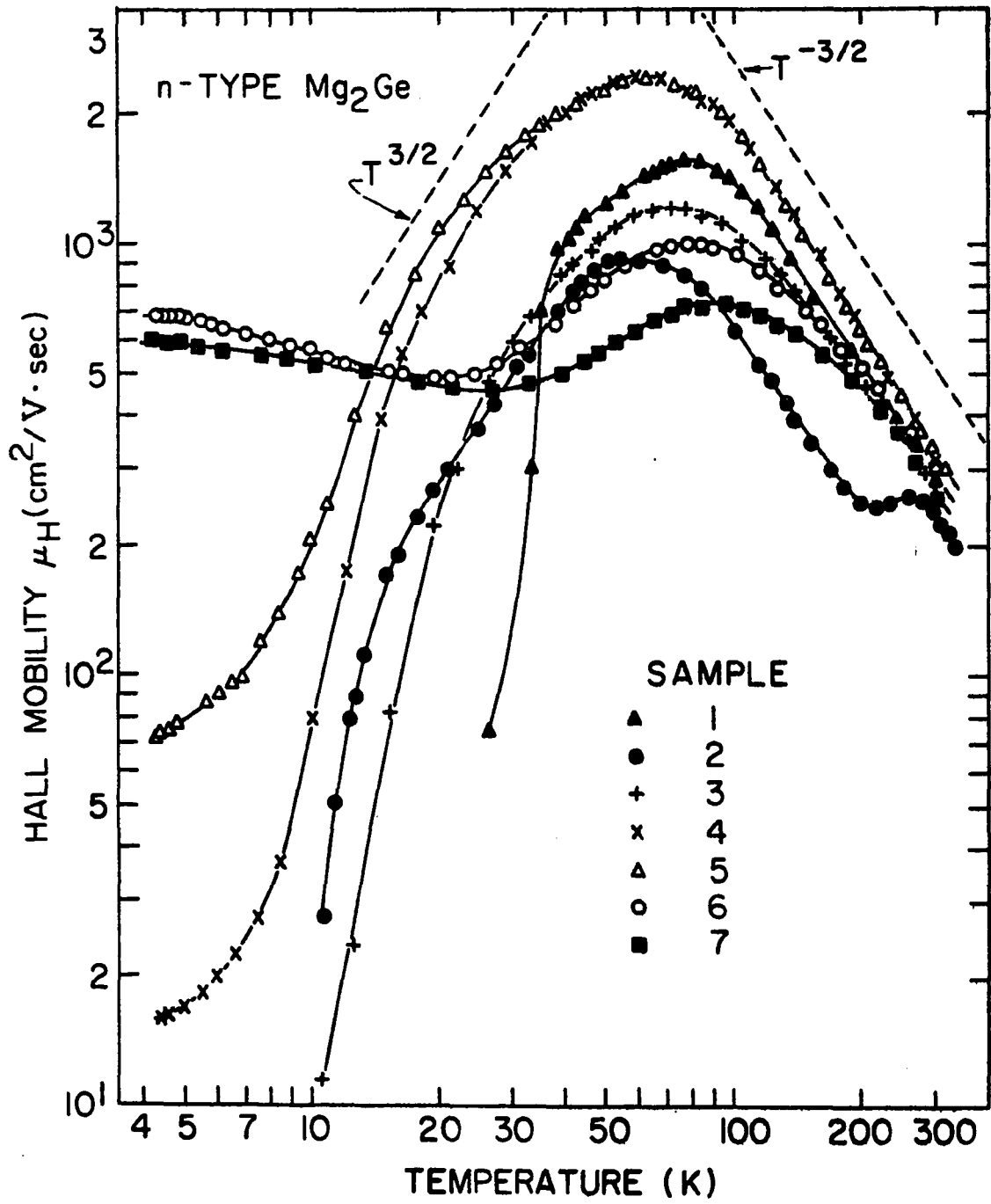
$$\mu_H = (\mu_c/b)(n_c b^2 + n_i)/(n_c b + n_i). \quad (4)$$

If $n_c \gg n_i$, $\mu_H = \mu_c$ and the mobility is the mobility of electrons in the conduction band. If $n_c \ll n_i$, $\mu_H = \mu_i$ and the mobility is the mobility of electrons in the impurity band. For the intermediate case Khosla²⁹ considers a large number of charge carriers to be in the impurity band, but a substantial fraction to be still in the conduction band. In this case $n_c b^2 > n_i > n_c b$. The mobility is then

$$\mu_H = \mu_c b(n_c/n_i). \quad (5)$$

From Eq. (5), the rapid decrease (greater than $T^{3/2}$) of the mobility

Fig. 4. Temperature dependence of the Hall mobility of Mg_2Ge from 4.2 K to 300 K. Sample 2 showed marked inhomogeneity in resistivity at 77 K, the other samples were quite homogeneous. For the homogeneous samples the Hall mobility from 150 K to 300 K had a $T^{-3/2}$ temperature dependence, which indicates that intravalley acoustic mode scattering is dominant in this temperature range and that the symmetry of the conduction band minima is X_3 rather than X_1 .



of sample 1 below 40 K, sample 3 below 30 K, and samples 2, 4, 5 below 20 K is attributed to the corresponding decrease of the ratio n_c/n_i in each sample. For samples 4 and 5 below 7 K, the mobilities tend to saturate. Below this temperature the majority of the electrons are in the impurity band and μ_H approaches the constant μ_i values.

A. Acoustic Mode Scattering

Some information regarding band structure and intervalley scattering can be deduced from the dependence of the Hall mobility on temperature (Fig. 4). From 150 K to 300 K the Hall mobilities show very nearly a $T^{-3/2}$ dependence upon temperature for all homogeneous samples (that is, all samples except sample 2). In this temperature range acoustic mode scattering is therefore dominant. Intervalley scattering is not important, since such scattering would, according to Harrison,³⁰ produce a stronger temperature dependence. Folland and Bassani⁴ have, from an examination of the selection rules, shown that small intervalley scattering (relative to intravalley scattering) would be expected in Mg_2X compounds near room temperature if the conduction band minima have a X_3 rather than X_1 symmetry. The band calculation of Mg_2Ge by Au-Yang and Cohen⁵ shows the conduction band minima to have X_3 symmetry which is consistent with our observation of small intervalley scattering.

Bardeen and Shockley³¹ have given a formula for the mobility limited by acoustic mode scattering. When modified for a many-valley semiconductor,³² the result is

$$\mu_A = \frac{(8\pi)^{1/2}}{9} \frac{e\hbar^4 d V_L^2}{(kT)^{3/2} (E_{1c})^2} \frac{(m_L^{*-1} + 2m_t^{*-1})}{(m_L^* m_t^{*2})^{1/2}}. \quad (6)$$

In this equation d is the density of the material and V_L is the longitudinal sound velocity. For Mg_2Ge , d is 3.10 g/cm^3 and V_L is $6.2 \times 10^5 \text{ cm/sec}$ according to Chung et al.³³ Our Hall mobility data at 300 K and Lee's effective masses² give a deformation potential for the conduction band of $|E_{1c}| = (18.7 \pm 0.9) \text{ eV}$. The deformation potential for the band gap E_1 may be estimated fairly well from the expression³⁴ $E_1 \approx -B(\partial E/\partial P)_T$, where B is the bulk modulus and $(\partial E/\partial P)_T$ is the pressure derivative of the band gap at constant temperature. For a cubic crystal³⁵ $B = (c_{11} + 2c_{12})/3$, and the elastic constants measured by Chung et al.³³ give $B = 5.46 \times 10^{11} \text{ dyn/cm}^2$. A value of $|(\partial E/\partial P)_T| < 5 \times 10^{-13} \text{ eV}\cdot\text{cm}^2/\text{dyn}$ has been reported for Mg_2Ge by Stella et al.¹¹ from the shift of the optical absorption edge with pressure. The maximum value of E_1 is thus estimated to be 0.27 eV . Since $|E_1| = |E_{1c}| - |E_{1v}|$ if E_{1c} and E_{1v} have the same sign,³⁶ and experimentally we find that $|E_{1c}|$ is much greater than $|E_1|$ the deformation potentials for the valence band E_{1v} and the conduction band E_{1c} must have the same sign and nearly the same magnitude.

B. Ionized Impurity Scattering

As shown in Table 1, samples 1, 2, and 3 are undoped samples. Their impurity carrier concentration may arise from small variations in stoichiometry of Mg_2Ge , but direct determination of such small

changes in stoichiometry appears to be impossible. Even for the Al-doped samples it is not possible to determine N_D directly from the atomic percent of aluminum which was added since there is a zone-refining effect during crystal growth which carries a substantial amount of the aluminum impurities to the top of the ingot. An attempt to determine the aluminum concentration with a mass spectrometer was not very successful. Interference from MgH and the high background level due to Mg were complicating factors. The mass spectrographic analysis of Mg_2Ge for impurities is shown in the Appendix (Table 5). For the nondegenerate samples 1-4 we can estimate the donor and acceptor concentrations N_D and N_A from the mobility curves (Figs. 4 and 5) between 50 K and 80 K.

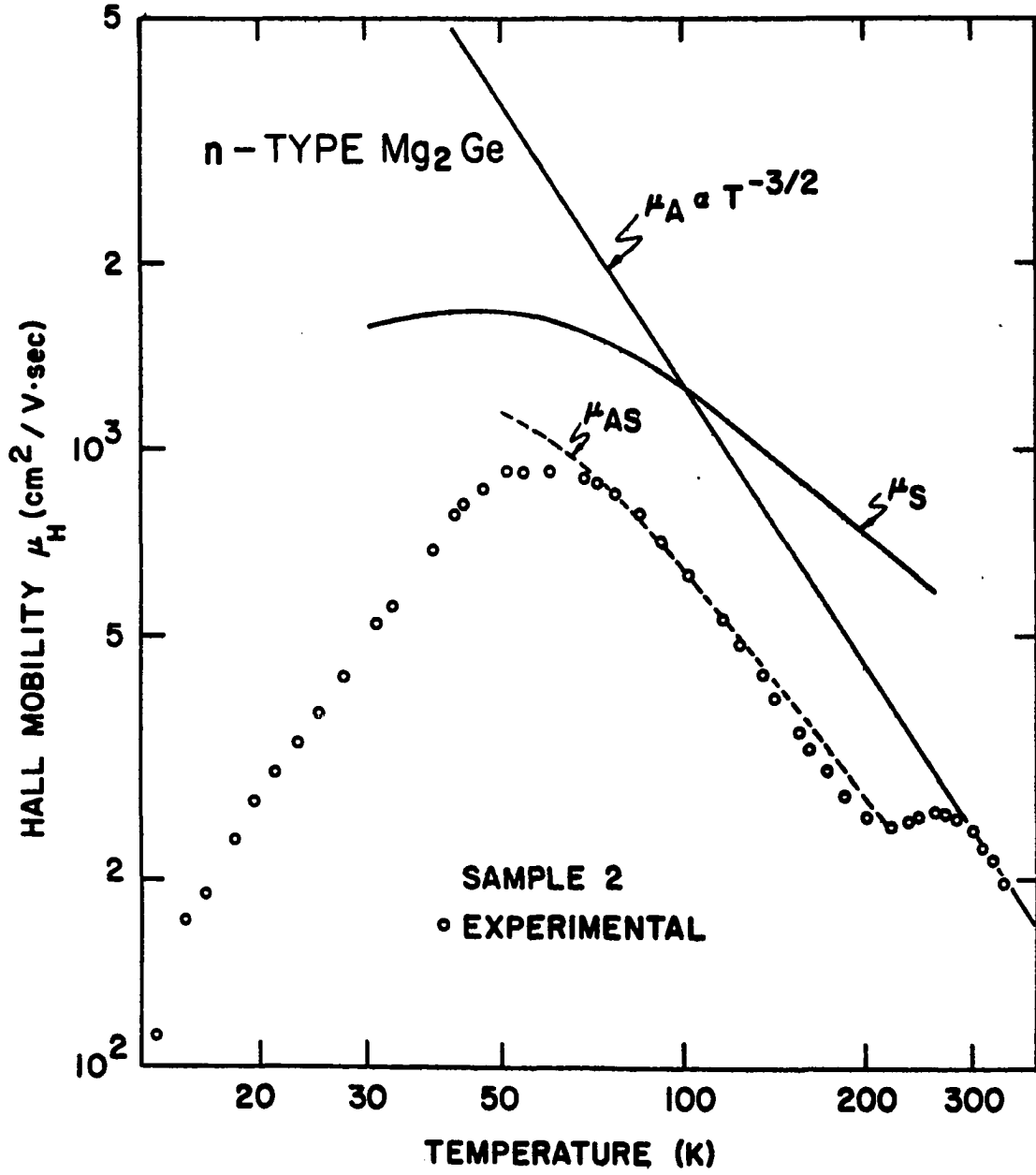
The maxima of the Hall mobilities of samples 3 and 4 were assumed to be limited by combinations of acoustic mode scattering and ionized impurity scattering. According to the Brooks-Herring³⁷ theory the mobility due to ionized impurity scattering is

$$\mu_1 = \frac{2^{7/2} (kT)^{3/2} \epsilon_0^2}{\pi^{3/2} e^3 m^{*1/2} (n+2N_A)} \left[\ln \left(\frac{6m^* (kT)^2 \epsilon_0}{\pi e^2 \hbar^2 n'} \right) - 1 \right]^{-1}, \quad (7)$$

where $n' = n + [1 - (n+N_A)/N_D](n+N_A)$. The expression

$$\mu_{AI}^{-1} = \mu_A^{-1} + \mu_1^{-1} \quad (8)$$

Fig. 5. The anomalous temperature dependence of the Hall mobility of sample 2, which was found to be homogeneous in resistivity at 300 K but inhomogeneous at 77 K. For temperatures greater than 300 K the mobility is limited only by acoustic mode scattering. For temperatures less than 200 K the mobility is limited by a combination of acoustic mode scattering and space charge scattering. The anomalous hump in the mobility curve between 200 K and 300 K occurs in the transition region.



was used to fit the maxima of the Hall mobilities. Using Lee's effective masses² and Eqs. (7) and (8), we determined N_D and N_A for samples 3 and 4. Values for N_D are given in Table 1, and N_A is the difference between N_D and n_0 . The donor and acceptor concentrations are comparable in magnitude.

C. Neutral Impurity Scattering

From Table 1, we see that sample 1 has an ionization energy ϵ_1 which is more than six times the ionization energy of any other sample. From Fig. 3, we observe that the number of charge carriers n in sample 1 is small below 100 K and the number of neutral impurity centers $N_N = (N_D - N_A) - n$ is large. Neutral impurity scattering will therefore be important in sample 1 at temperatures below 100 K. The expression obtained by Erginsoy³⁸ for the mobility due to neutral impurity scattering is

$$\mu_N = e^3 m^{*3} / 20\hbar^3 \epsilon_0 N_N, \quad (9)$$

where $m^* = (m_l^* m_t^{*2})^{1/3}$ is a mean effective mass. A composite result of mobility due to acoustic mode, ionized, and neutral impurity scatterings, obtained from the expression

$$\mu_{AIN}^{-1} = \mu_A^{-1} + \mu_I^{-1} + \mu_N^{-1}, \quad (10)$$

was used to fit the mobility curve of sample 1 near the maximum (60 K). Using Lee's effective masses² and Eqs. (7), (9), and (10), we obtained

$N_D = 8.4 \times 10^{16} \text{ cm}^{-3}$ and $N_A = 1.7 \times 10^{16} \text{ cm}^{-3}$. In spite of its very high resistivity and Hall coefficient below 100 K, sample 1 does not have an exceptionally high electron mobility owing to scattering of the electrons by neutral impurities.

D. Space Charge Scattering

Since space charge scattering owing to local inhomogeneities can greatly affect the mobility,³⁹ the homogeneity of each sample must be taken into consideration when we analyze the Hall mobility data. Among these seven samples, only sample 2 showed marked inhomogeneity at 77 K. The other samples were quite homogeneous, since the resistivities showed less than 10% variation along the length of each sample when measured either at 300 K or at 77 K.

Sample 2 showed abnormal behavior in that it had a hump between 200 K and 300 K in its mobility curve (see Fig. 4 and 5). A test of the homogeneity of sample 2 was revealing. Although its resistivity varied less than 30% along the sample at 300 K, its resistivity changed as much as an order of magnitude along the sample at 77 K. As suggested by Weisberg³⁹ the Hall mobility in semiconductors can be greatly reduced by inhomogeneous impurity distributions, owing to the formation of large space charge regions surrounding the local inhomogeneities. For the mobility limited by space charge scattering he gives the equation

$$\mu_S = A(n/n_{300})^{1/3} (T/300)^{-5/6}, \quad (11)$$

where n_{300} is the carrier concentration at 300 K, and n is the carrier concentration at the temperature T . The constant A must be determined experimentally for each particular position of the probes.

The mobility curve of sample 2 can be explained in the following way. For temperatures higher than 300 K the mobility is mainly limited by acoustic mode scattering. For temperatures below 200 K the inhomogeneity of the impurity distribution produces space charge scattering which must be added to the acoustic mode scattering. For $A = 626 \text{ cm}^2/\text{V}\cdot\text{sec}$, the mobility μ_S obtained from Eq. (11) for sample 2 is shown in Fig. 5. The combined contribution from acoustic mode scattering and space charge scattering, which is

$$\mu_{AS}^{-1} = \mu_A^{-1} + \mu_S^{-1}, \quad (12)$$

gives a good fit to the experimental mobility data from 200 K down to 70 K as shown in Fig. 5. The anomalous hump in the mobility curve between 200 K and 300 K occurs in the transition region. We see that space charge scattering is very important below 200 K, but not important above 300 K.

In Fig. 5, a composite mobility due to acoustic mode scattering, space charge scattering, and ionized impurity scattering was used to fit the mobility maximum of sample 2 from the expression

$$\mu_{ASI}^{-1} = \mu_{AS}^{-1} + \mu_I^{-1}. \quad (13)$$

From Eqs. (13) and (7), and Lee's effective masses,² we found the donor

concentration N_D in sample 2 to be $1.4 \times 10^{16} \text{ cm}^{-3}$. Of all our samples, sample 2 had the lowest donor concentration.

VII. MAGNETORESISTANCE

A. Theoretical Considerations

For the past two decades the weak-field magnetoresistance of semiconductors has been studied extensively both experimentally and theoretically. For a cubic crystal in a weak magnetic field Pearson and Suhl⁴⁰ have shown that the resistivity increment $\Delta\rho = \rho(H) - \rho(0)$ due to the presence of a magnetic field \vec{H} is given by the equation

$$\Delta\rho/\rho_0 H^2 = b + c (\vec{T} \cdot \vec{H})^2 / l^2 H^2 + d(l_1^2 H_1^2 + l_2^2 H_2^2 + l_3^2 H_3^2) / l^2 H^2,$$

$$\mu_H H \ll 10^8, \quad (14)$$

where the constants b , c , and d are the magnetoresistance coefficients, ρ_0 is the zero-field resistivity, \vec{T} is the current, and the subscripts 1, 2, 3 represent the three axes of the crystal. The Hall mobility μ_H is measured in $\text{cm}^2/\text{V}\cdot\text{sec}$, and the magnetic field H is measured in oersteds. Equation (14) applies only to crystals having point group symmetry⁴¹ $m\bar{3}m$, 432 , or $\bar{4}3m$. (Mg_2Ge belongs to the point group $m\bar{3}m$.) If the direction cosines of \vec{T} and \vec{H} referred to the crystal axes are i, j, k , and l, m, n then Eq. (14) becomes⁴⁰

$$\Delta\rho/\rho_0 H^2 = b + c (il + jm + kn)^2 + d(i^2 l^2 + j^2 m^2 + k^2 n^2). \quad (15)$$

For the special sample orientation shown in Fig. 1, the current vector \vec{T} is along the direction $[\bar{1}\bar{1}2]$, and the angle θ specifies the direction of \vec{H} relative to $[\bar{1}\bar{1}2]$. The direction cosines can then be specified as $-1/\sqrt{6}$, $-1/\sqrt{6}$, $2/\sqrt{6}$ for \vec{T} and $(\sqrt{2} \sin \theta - \cos \theta)/\sqrt{6}$, $(\sqrt{2} \sin \theta - \cos \theta)/\sqrt{6}$, $(\sqrt{2} \sin \theta + 2 \cos \theta)/\sqrt{6}$ for \vec{H} . Equation (15) then becomes⁴²

$$\Delta\rho/\rho_0 H^2 = (12b + 6c + 5d)/12 + (1/12)(6c + d) \cos 2\theta + (d/3\sqrt{2}) \sin 2\theta. \quad (16)$$

Equation (16) allows all three magnetoresistance coefficients b , c , and d to be obtained from the measurement of $\Delta\rho/\rho_0 H^2$ as a function of the angle θ .

In the many-valley model of a semiconductor, b , c , and d depend on the Hall mobility μ_H , the anisotropy parameter K , and the relaxation time τ . All of these quantities depend upon the scattering mechanism. As suggested by Herring and Vogt,⁴³ who take into account anisotropy in the scattering process, the main effects of scattering on the distribution function over each spheroidal constant energy surface can be described by two relaxation times, one transverse $\tau_t(\epsilon)$ and one longitudinal $\tau_l(\epsilon)$ to the axis of revolution of the spheroid. To simplify the analysis we assume⁴⁴ the relaxation times have the same dependence on energy

$$\tau_L = \tau_L^0 \tau(\epsilon) \quad \text{and} \quad \tau_t = \tau_t^0 \tau(\epsilon). \quad (17)$$

The relaxation time anisotropy $K_\tau \equiv \tau_L/\tau_t = \tau_L^0/\tau_t^0$, which takes into account the possibility of anisotropy scattering, is then independent of energy. The anisotropy parameter K , which can be represented by the ratio of the mass anisotropy to the relaxation time anisotropy,

$$K \equiv K_m/K_\tau = (m_L^*/m_t^*)/(\tau_L^0/\tau_t^0) \quad (18)$$

is also independent of energy. Under these assumptions the coefficients b , c , and d for a cubic semiconductor, having $\langle 100 \rangle$ type spheroids, are shown in Table 2.¹⁵ Here $\langle \tau^n \rangle$ represents the Maxwellian average for the n th power of the relaxation time $\tau(\epsilon) = \mu \epsilon^p$, where μ is a constant and p is determined by the scattering mechanism.⁴⁵ The comprehensive review by Beer⁴⁴ gives the specific relationship of the coefficients b , c , and d to the symmetry of the constant energy spheroids in the Brillouin zone.

$$\begin{aligned} \text{Spherical symmetry:} & \quad b + c = 0, \quad d = 0 \\ \langle 100 \rangle \text{ type spheroids:} & \quad b + c + d = 0, \quad d < 0 \\ \langle 111 \rangle \text{ type spheroids:} & \quad b + c = 0, \quad d > 0 \\ \langle 110 \rangle \text{ type spheroids:} & \quad b + c - d = 0, \quad d > 0 \end{aligned} \quad (19)$$

Therefore, a determination of the coefficients b , c , and d allows us to obtain the orientation of the constant energy spheroids in a many-valley semiconductor.

Table 2. Magnetoresistance coefficients in terms of the Hall mobility, anisotropy parameter, and relaxation time for $\langle 100 \rangle$ type constant energy spheroids.¹⁵

Magnetoresistance Coefficients	For $\langle 100 \rangle$ Type Spheroids
b	$\mu_H^2 \left[\frac{\langle \tau \rangle \langle \tau^3 \rangle}{\langle \tau^2 \rangle^2} \frac{(2K+1)(K^2+K+1)}{K(K+2)^2} - 1 \right]$
c	$\mu_H^2 \left[1 - \frac{\langle \tau \rangle \langle \tau^3 \rangle}{\langle \tau^2 \rangle^2} \frac{3(2K+1)}{(K+2)^2} \right]$
d	$- \mu_H^2 \frac{\langle \tau \rangle \langle \tau^3 \rangle}{\langle \tau^2 \rangle^2} \frac{(2K+1)(K-1)^2}{K(K+2)^2}$
b + c + d	0

Dimensionless Seitz coefficients have been suggested by Allgaier⁴⁶ in order to simplify the comparison of results when one uses different samples, different temperatures or different semiconductors. Table 2 shows that the square of the mobility μ_H^2 is a common factor of the magnetoresistance coefficients b, c, and d. We can, therefore, write Eq. (15) in the form

$$\begin{aligned} (\Delta\rho/\rho_0)/(\mu_H H/C)^2 = & b' + c' (1 + jm + kn)^2 \\ & + d' (l^2 + m^2 + n^2), \end{aligned} \quad (20)$$

where $C = 10^8 \text{ cm}^2 \text{ Oe/V}\cdot\text{sec}$ and b' , c' , and d' are now the dimensionless Seitz coefficients.

In compound semiconductors, it is highly desirable to use a single sample to obtain all three coefficients b, c, and d. Otherwise slight variations in stoichiometry and nonuniform distributions of impurities, which occur from one sample to another, will produce different values of μ_H and make the interpretation of the data difficult. Also, magnetoresistance measurements are very sensitive to inhomogeneities as pointed out by Herring⁴⁷ and by Bate et al.⁴⁸ For these reasons, we have used just one sample at each impurity concentration to determine the coefficients b, c, and d; and we have carefully checked the homogeneity of all samples not only at 300 K but also at 77 K.

B. Results and Analysis

The magnetic field dependence up to 8 kOe of both the longitudinal ($\vec{T} \parallel \vec{H}$) and transverse ($\vec{T} \perp \vec{H}$) magnetoresistance $\Delta\rho/\rho_0$ was determined for all seven samples at 77.4 K. Sample 4 was also measured at 43.6 K. As shown in Fig. 6, both the longitudinal and transverse effects for each sample show the normal H^2 dependence as expected in weak magnetic fields ($\mu_H H \ll 10^8$). A much higher magnetic field strength would be required to violate the weak-field inequality, since the maximum value of μ_H for our samples is only $2.5 \times 10^3 \text{ cm}^2/\text{V}\cdot\text{sec}$.

The quantity $\Delta\rho/\rho_0 H^2$ was measured as a function of the angle θ for seven homogeneous n-type Mg_2Ge samples at 77.4 K. The data are shown in Figs. 7 and 8. Since the typical value of the magnetoresistance $\Delta\rho/\rho_0$ is about 10^{-3} for our samples, and the zero-field resistivity ρ_0 is very sensitive to variations in temperature, it was important to keep the sample temperature stable. Therefore, the magnetoresistance effect was measured at several stable temperatures by using suitable refrigerants. Liquid nitrogen was excellent for one such temperature. Liquid helium was not satisfactory because of impurity band conduction at this temperature. Besides liquid nitrogen temperature and room temperature, a stable temperature at 194.5 K was provided by dry ice in acetone, and a fairly stable temperature at 43.6 K by pumping on liquid nitrogen. For sample 4 we measured $\Delta\rho/\rho_0 H^2$ versus θ at these four stable temperatures. The results are shown in Fig. 8.

From the angular dependence of $\Delta\rho/\rho_0 H^2$ shown in Figs. 7 and 8, the magnetoresistance coefficients b , c , and d for each sample

Fig. 6. The longitudinal and transverse magnetoresistance $\Delta\rho/\rho_0$ of seven samples of Mg_2Ge , which show the normal H^2 magnetic field dependence for H up to 8 kOe. The symbol L represents longitudinal ($\vec{T} \parallel \vec{H}$) and the symbol T represents transverse ($\vec{T} \perp \vec{H}$) magnetoresistance.

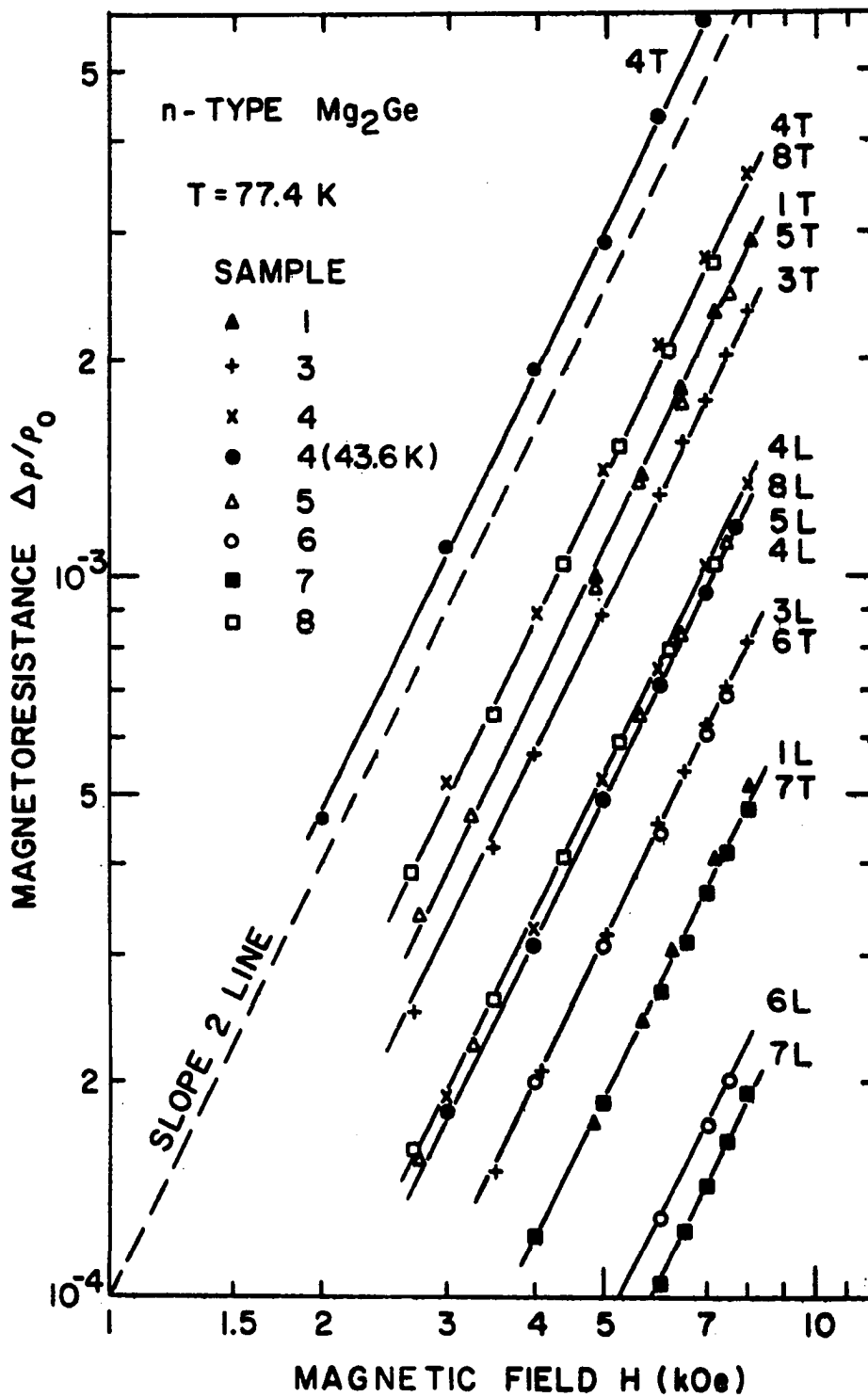


Fig. 7. The magnetoresistance effect in Mg_2Ge showing the angular dependence of $\Delta\rho/\rho_0 H^2$ at 77 K. For each sample $\Delta\rho/\rho_0 H^2$ is described by Eq. (16), and a set of magnetoresistance coefficients b , c , and d can be obtained from each curve. Since $b + c + d = 0$ and $d < 0$ we conclude that n-type Mg_2Ge is a many-valley semiconductor with constant energy spheroids in the $\langle 100 \rangle$ directions.

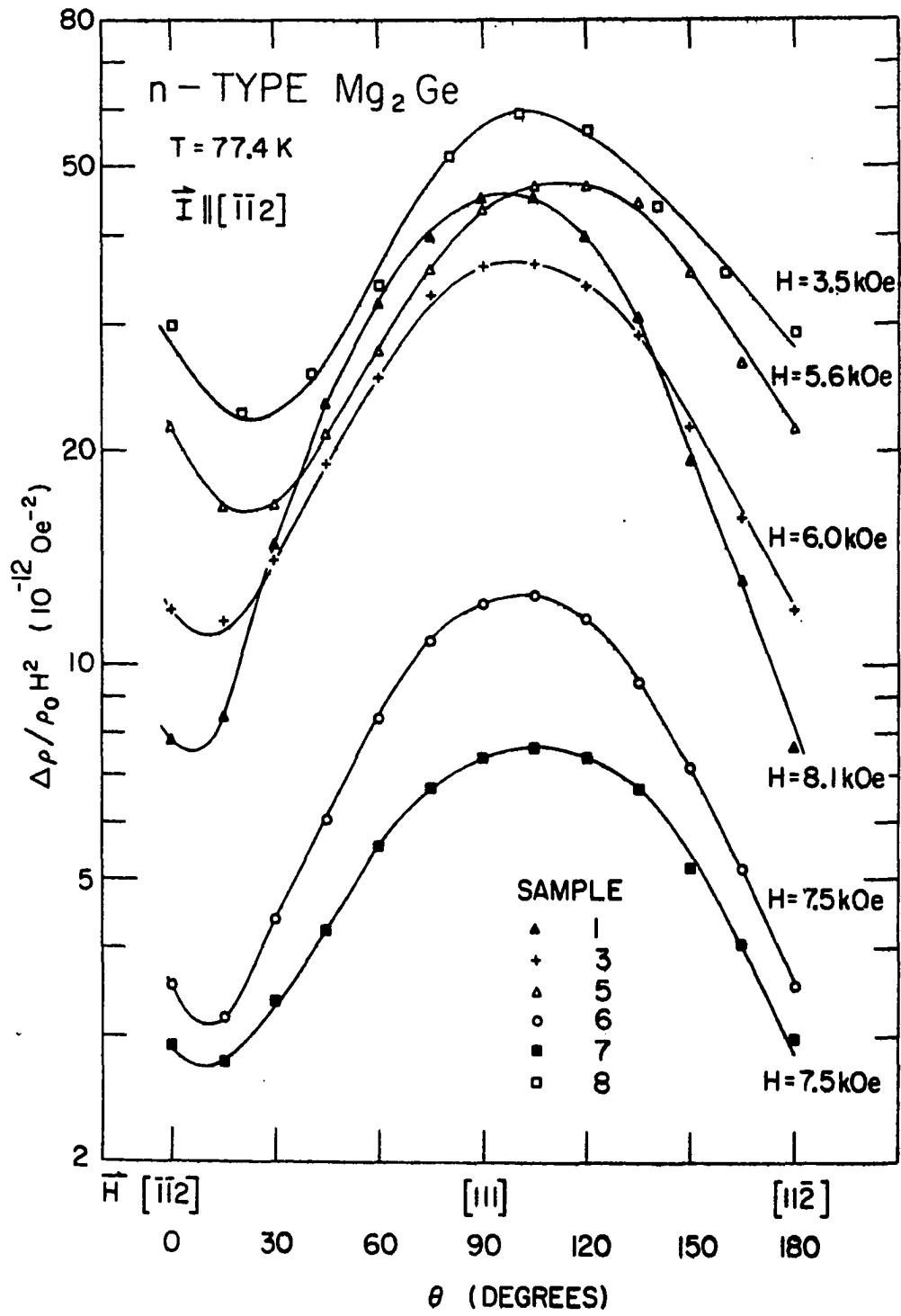
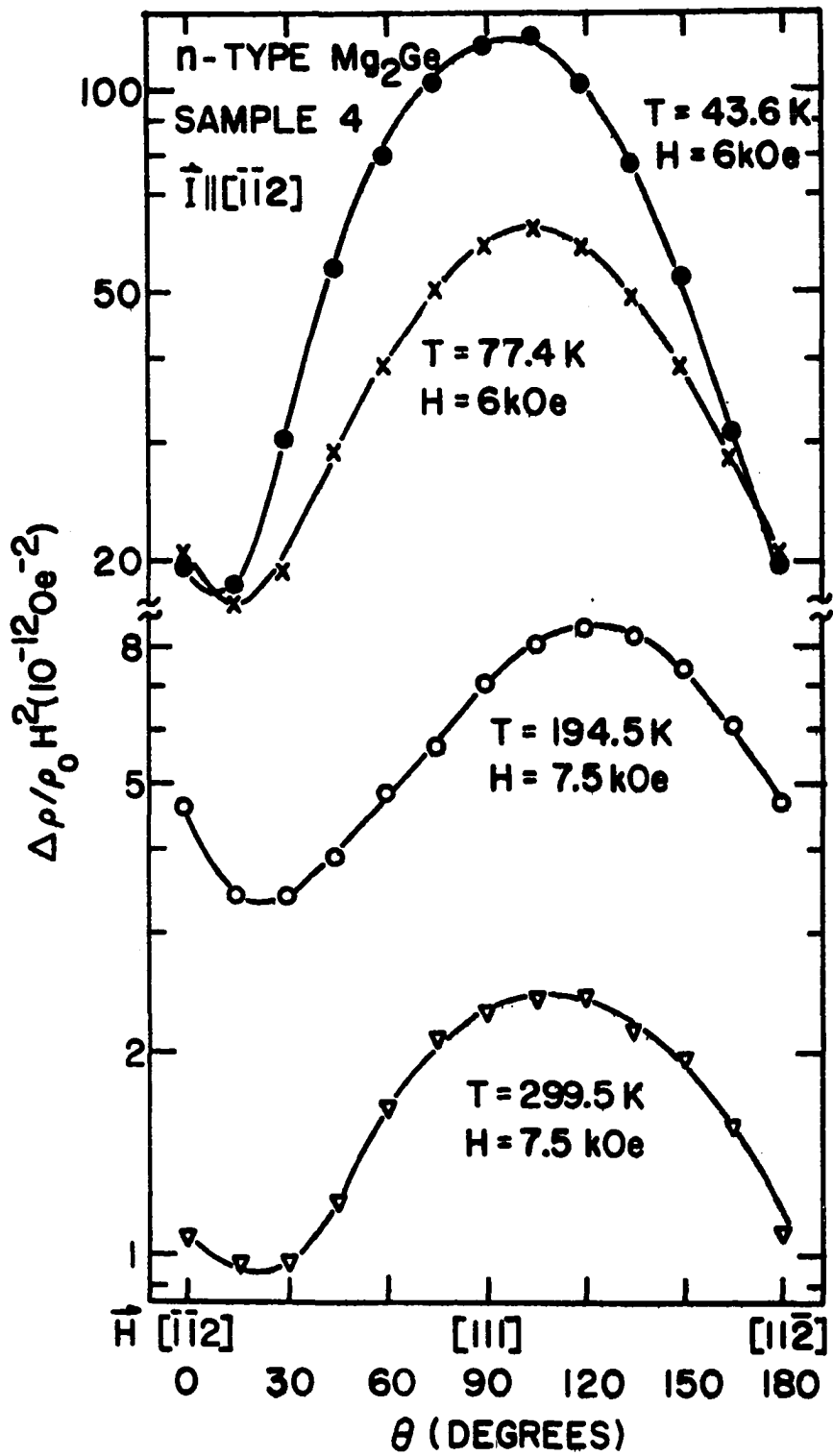


Fig. 8. The magnetoresistance effect in Mg_2Ge showing the angular dependence of $\Delta\rho/\rho_0 H^2$ for sample 4 at four stable temperatures. The symmetry condition for $\langle 100 \rangle$ type spheroids is satisfied at all four temperatures. The values of the anisotropy parameter K were found to decrease from 2.13 at 299.5 K to 1.65 at 43.6 K.



were determined. A computer was used to minimize the rms deviation from Eq. (16). Values for b , c , and d are shown in Table 3.

The coefficients b , c , and d satisfy the symmetry condition $b + c + xd = 0$, $d < 0$ with $x \approx 1$. As shown in Table 3, the value of x varied from 0.900 to 1.09. In all samples, therefore, x was within 10 percent of the theoretical value $x = 1$. The condition for $\langle 100 \rangle$ type spheroids is well satisfied for all samples at 77.4 K and for sample 4 also at 43.6 K, 194.5 K and 299.5 K. This result confirms the theoretical predictions of Lee,² Folland and Bassani,⁴ and Au-Yang and Cohen⁵ that the conduction band minima of Mg_2Ge consist of a set of constant energy spheroids along the $\langle 100 \rangle$ directions in the Brillouin zone.

For $\langle 100 \rangle$ type spheroids we can obtain the anisotropy parameter K from Table 2 by eliminating the factor $\langle \tau \rangle \langle \tau^3 \rangle / \langle \tau^2 \rangle^2$

$$\frac{2(K - 1)^2}{K^2 + K + 1} = \frac{b + c - d}{b + \mu_H^2}. \quad (21)$$

From Eq. (21) and the values of b , c , d , and μ_H in Table 3 we determined K . The values for our seven samples are given in Table 3.

For each value of K the scattering factor $\langle \tau \rangle \langle \tau^3 \rangle / \langle \tau^2 \rangle^2$ (see Table 2) was computed from the values of μ_H and b , μ_H , and c , and μ_H and d listed in Table 3. These three values for each scattering factor were always within 3 percent of the average value which is given in the last column of Table 3.

Table 3. The magnetoresistance coefficients b, c, and d, the dimensionless Seitz coefficients, b', c', and d', the anisotropy parameter K, and the scattering factor $\langle \tau \rangle \langle \tau^3 \rangle / \langle \tau^2 \rangle^2$ of n-type Mg₂Ge.

Sample No.	T (K)	$-R_H$ ($10^2 \text{ cm}^3/\text{C}$)	ρ_0 ($10^{-2} \Omega \text{ cm}$)	μ_H ($10^2 \text{ cm}^2/\text{V sec}$)	b	c (10^{-12} Oe^{-2})	d
1	77.4	199.0	1250.0	15.9	50.7	-34.5	-16.4
3	77.4	7.64	60.2	12.7	42.7	-20.8	-20.2
4	43.6	3.45	16.3	21.2	132.0	-88.8	-48.0
	77.4	1.95	8.71	22.4	73.7	-30.6	-45.3
	194.5	1.57	23.1	6.80	12.3	-2.81	-9.44
	299.5	1.48	47.2	3.14	2.91	-0.74	-2.07
5	77.4	0.834	3.74	22.3	58.5	-14.2	-46.8
6	77.4	0.174	1.74	10.0	14.5	-7.34	-7.30
7	77.4	0.0996	1.36	7.32	9.14	-3.64	-5.06
8	77.4	2.84	12.0	23.7	69.4	-19.5	-46.7

x	b'	c'	d'	K		$\langle \tau \rangle \langle \tau^3 \rangle / \langle \tau^2 \rangle^2$	
				prolate	oblate	prolate	oblate
0.988	0.201	-0.137	-0.065	1.51	0.664	1.16	1.16
1.08	0.265	-0.129	-0.125	1.78	0.560	1.17	1.15
0.900	0.295	-0.198	-0.107	1.65	0.606	1.26	1.24
0.951	0.147	-0.061	-0.090	1.64	0.610	1.10	1.09
1.01	0.266	-0.061	-0.204	2.10	0.475	1.14	1.11
1.05	0.296	-0.075	-0.211	2.13	0.470	1.16	1.12
0.946	0.118	-0.029	-0.094	1.67	0.599	1.07	1.06
0.981	0.145	-0.073	-0.073	1.56	0.640	1.11	1.09
1.09	0.170	-0.068	-0.094	1.68	0.595	1.09	1.08
1.05	0.124	-0.035	-0.083	1.63	0.611	1.07	1.05

The scattering factor is always greater than one as required by the Schwartz inequality $\langle \tau \rangle \langle \tau^3 \rangle / \langle \tau^2 \rangle^2 \geq 1$. Our experimental values, which vary from 1.05 to 1.26, have very reasonable magnitudes. The theoretical values are 1.27 for acoustical mode scattering, 1.00 for neutral impurity scattering, and 1.58 for ionized impurity scattering.

In solving for $K = K_m / K_\tau$ we assumed the constant energy surfaces were prolate ($K > 1$) rather than oblate ($K < 1$), since the theoretical value for K_m from Table 1 of Lee's paper² is 2.52 and the value of K_τ according to Fig. 12 of Herring's paper⁴⁹ is probably not far from one when intravalley acoustic mode scattering is dominant. At 77 K the values of K for our samples ranged from 1.51 to 1.78. The K values for Mg_2Ge are smaller than the K values for some other semiconductors such as n-type Ge ($K \approx 8$ at 77 K) reported by Laff and Fan,⁵⁰ n-type Si ($K = 4.6$ at 68 K) measured by Pearson and Herring,⁵¹ n-type Si ($K = 5.2$ at 80 K) measured by Broudy and Venables,⁵² and n-type Mg_2Sn ($K = 2.8$ to 3.53 at 77 K) determined by Umeda.⁹

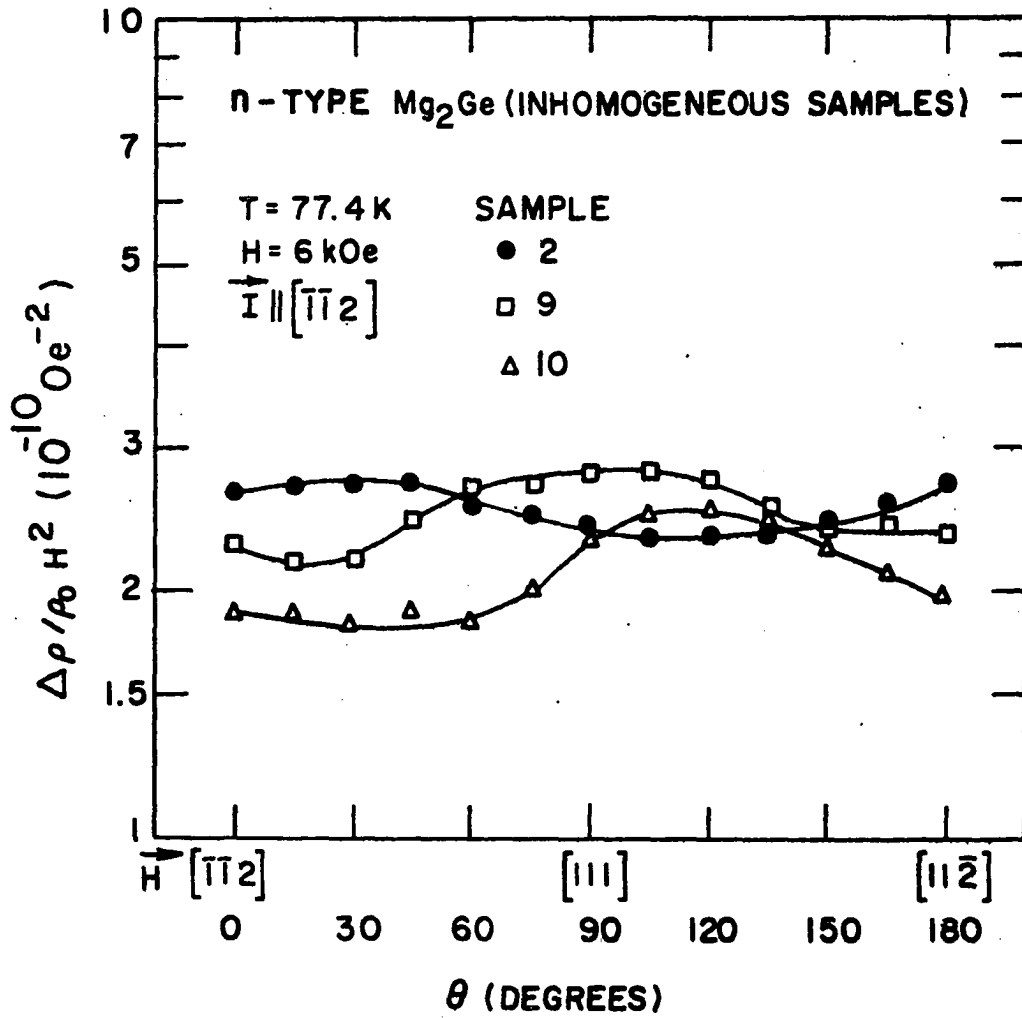
At 77 K the value of $\Delta\rho/\rho_0 H^2$ in Mg_2Ge is quite small for a semiconductor. It is about the same order of magnitude as that observed for indium oxide by Weiher and Dick.⁵³ It is about one order of magnitude smaller than $\Delta\rho/\rho_0 H^2$ observed by Umeda⁹ in Mg_2Sn , and about two orders of magnitude smaller than $\Delta\rho/\rho_0 H^2$ observed in Ge by Pearson and Suhl.⁴⁰ The small magnetoresistance effect in Mg_2Ge is the result of small Hall mobility μ_H . In fact, if we look at the dimensionless Seitz coefficients, related to $(\Delta\rho/\rho_0)/(\mu_H H/C)^2$ by Eq. (20), we see values which are comparable to those of other

semiconductors such as PbTe (Allgaier⁴⁶) or SrTiO₃ (Frederikse et al.⁵⁴). Also these coefficients b', c', d' (as shown in Table 3) are not very different for different samples or different temperatures. This uniformity suggests that our data are consistent and reliable.

The anisotropy parameter K for sample 4 was obtained at the four temperatures 299.5 K, 194.5 K, 77.4 K, and 43.6 K. The results are shown in Table 3. The value of $K = K_m/K_T$ decreased from 2.13 at 300 K to 1.65 at 43.6 K. This decrease is to be expected, as emphasized by Laff and Fan,⁴⁹ since scattering by ionized impurities becomes more important at lower temperatures. Mg₂Ge does not have a small direct energy gap^{5,12} and thus the shape of the spheroids can not be very sensitive to temperature. Hence K_m should be nearly constant. The decrease in K, therefore, means an increase in K_T . If we assume K_T at 300 K to be approximately one, since intravalley acoustic mode scattering is dominant at this temperature, then K_T at 43.6 K is 1.29. Also K_m at 300 K would be about 2.1 which is not greatly different from the theoretical estimate of 2.5 by Lee.² Our value is certainly a rough estimate and Lee's value depends upon his effective masses which are uncertain because the symmetry of the conduction band minima is X_3 , as predicted by Au-Yang and Cohen⁵ and concluded from our Hall mobility temperature dependence, rather than X_1 as calculated by Lee.²

Figure 9 shows $\Delta\rho/\rho_0 H^2$ versus θ at 77 K for three inhomogeneous n-type Mg₂Ge samples. Our resistivity tests for these samples at 77 K revealed variations in resistivities greater than a factor of 2 along

Fig. 9. The magnetoresistance effect of Mg_2Ge showing the angular dependence of $\Delta\rho/\rho_0H^2$ at 77 K for three inhomogeneous samples. Values of $\Delta\rho/\rho_0H^2$ are about an order of magnitude higher than the values for homogeneous samples shown in Fig. 7. $\Delta\rho/\rho_0H^2$ was insensitive to the angle θ between \vec{l} and \vec{H} in sharp contrast to the effects observed with homogeneous samples (Figs. 7 and 8).



each sample. $\Delta\rho/\rho_0 H^2$ at 77 K for these samples is about an order of magnitude higher than for our homogeneous samples. This result is not too surprising, since an anomalously high magnetoresistance effect for inhomogeneous samples of InSb has been observed by Bate et al.⁴⁸ The Hall mobility at 77 K for these inhomogeneous samples 2, 9, and 10 is $8.6 \times 10^2 \text{ cm}^2/\text{cmV}\cdot\text{sec}$, $2.2 \times 10^3 \text{ cm}^2/\text{V}\cdot\text{sec}$, and $2.5 \times 10^3 \text{ cm}^2/\text{V}\cdot\text{sec}$, respectively. Despite the large differences in Hall mobility of these samples the magnetoresistances are practically the same. Also, $\Delta\rho/\rho_0 H^2$ is insensitive to the angle θ , in sharp contrast to the results for our homogeneous samples shown in Figs. 7 and 8, where the values of $\Delta\rho/\rho_0 H^2$ are quite sensitive to the angle θ and to the Hall mobility μ_H . These facts imply that Eq. (16) can not be applied to these inhomogeneous samples. In homogeneous samples give anomalous magnetoresistance effects and should not be used to determine the electronic structure of a semiconductor.

VIII. CONCLUSIONS

Weak-field magnetoresistance measurements have been made on homogeneous single crystals of n-type Mg_2Ge . Our results confirm the theoretical prediction that n-type Mg_2Ge is a many-valley semiconductor with constant energy spheroids in the $\langle 100 \rangle$ directions. The Hall mobility of our samples from 150 K to 300 K had a $T^{-3/2}$ temperature dependence, which indicates that intravalley acoustic mode scattering is the dominant scattering mechanism in this temperature range and that the symmetry of the conduction band minima is X_3 rather than X_1 .

The anisotropy parameter $K = K_m/K_T$ was found to be about 2.1 at 300 K. If we assume the relaxation time anisotropy K_T to be approximately one at 300 K, since intravalley acoustic mode scattering is dominant at this temperature, the effective mass ratio K_m will also be about 2.1. This K_m value is not greatly different from the theoretical estimate² of 2.5.

We have carefully checked the homogeneity of each sample at 300 K and 77 K. Inhomogeneous samples showed anomalies in the Hall mobility temperature dependence, and also showed higher magnetoresistance. Values of $\Delta\rho/\rho_0 H^2$ were insensitive to the Hall mobility and to the angle between \vec{T} and \vec{H} in sharp contrast to the effects observed with homogeneous samples.

It would be desirable to make piezoresistance measurements on Mg_2Ge . A combination of such measurements with our values of the anisotropy parameter could yield the deformation potential $\frac{P}{u}$.⁸

The piezoresistance effect will probably be smaller for Mg_2Ge than for Mg_2Sn due to the smaller K value for Mg_2Ge . It might also be desirable to study the magnetoresistance and piezoresistance of p-type Mg_2Ge since little experimental data are available on the electronic structure of p-type material.

IX. LITERATURE CITED

1. R. D. Redin, R. G. Morris, and G. C. Danielson, Phys. Rev. 109, 1916 (1958).
2. P. M. Lee, Phys. Rev. 135, A1110 (1964).
3. N. O. Folland, Phys. Rev. 158, 764 (1967).
4. N. O. Folland and F. Bassani, J. Phys. Chem. Solids 29, 281 (1968).
5. M. Y. Au-Yang and M. L. Cohen, Phys. Rev. 178, 1358 (1969).
6. J. P. Van Dyke and F. Herman, Phys. Rev. B 2, 1644 (1970).
7. W. B. Whitten and G. C. Danielson, in Proceedings of the Seventh International Conference on the Physics of Semiconductors, edited by M. Hulin (Dunod, Paris, 1964), p. 537.
8. L. D. Crossman and G. C. Danielson, Phys. Rev. 171, 867 (1968).
9. J. Umada, J. Phys. Soc. Japan 19, 2052 (1964).
10. G. A. Stringer and R. J. Higgins, J. Appl. Phys. 41, 489 (1970).
11. A. Stella, A. D. Brothers, R. H. Hopkins, and D. W. Lynch, Phys. Status Solidi 23, 697 (1967).
12. L. A. Lott and D. W. Lynch, Phys. Rev. 141, 681 (1966).
13. D. H. Grotzky and P. H. Sidles, USAEC Report No. IS-2100, July, 1969, p. P-53 (unpublished).
14. R. G. Schwartz, H. Shanks, and B. C. Gerstein, J. Solid State Chem. 3, 533 (1971).
15. M. Glicksman, in Progress in Semiconductors, edited by A. F. Gibson et al. (Wiley, New York, 1958), Vol. 3, pp. 3-25.
16. S. N. Lee, Ph. D. thesis (Iowa State University, 1968) (unpublished).
17. F. R. Kroeger and W. A. Rhinehart, Rev. Sci. Instr. 42, 1532 (1971).
18. H. Fritzsche, Phys. Rev. 99, 406 (1955).
19. A. Miller and E. Abrahams, Phys. Rev. 120, 745 (1960).

20. N. F. Mott and W. D. Twose, *Advan. Phys.* 10, 107 (1961).
21. H. Nishimura, *Phys. Rev.* 138, A815 (1965).
22. E. A. Davis and W. D. Compton, *Phys. Rev.* 140, A2183 (1965).
23. H. Brooks, in Advances In Electronics and Electron Physics, Vol. VII, edited by L. Marton (Academic, New York, 1955), pp. 102-104.
24. D. McWilliams and D. W. Lynch, *Phys. Rev.* 130, 2248 (1963).
25. T. N. Morgan, *Phys. Rev.* 139, A343 (1965).
26. C. S. Hung and J. R. Gliessman, *Phys. Rev.* 96, 1226 (1954).
27. E. M. Conwell, *Phys. Rev.* 103, 51 (1956).
28. H. C. Casey, Jr., F. Ermanis, and K. B. Wolfstirn, *J. Appl. Phys.* 40, 2945 (1969).
29. R. P. Khosla, *Phys. Rev.* 183, 695 (1969).
30. W. A. Harrison, *Phys. Rev.* 104, 1281 (1956).
31. J. Bardeen and W. Shockley, *Phys. Rev.* 80, 72 (1950).
32. R. A. Smith, Semiconductors (Cambridge U.P., Cambridge, England, 1961), p. 147.
33. P. L. Chung, W. B. Whitten, and G. C. Danielson, *J. Phys. Chem. Solids* 26, 1753 (1965).
34. E. Ehrenreich, *Phys. Rev.* 120, 1951 (1960).
35. C. Kittel, Introduction to Solid State Physics (Wiley, New York, 1967), 3rd ed., p. 118.
36. W. Shockley, Electrons and Holes In Semiconductors (Van Nostrand, New York, 1950), p. 270.
37. F. J. Blatt, in Solid State Physics, Vol. 4, edited by F. Seitz and D. Turnbull (Academic, New York, 1957), p. 344.
38. C. Erginsoy, *Phys. Rev.* 79, 1013 (1950).
39. L. R. Weisberg, *J. Appl. Phys.* 33, 1817 (1962).
40. G. L. Pearson and H. Suhl, *Phys. Rev.* 83, 768 (1951).

41. A. C. Beer, Solid State Physics - Supplement 4, edited by F. Seitz and D. Turnbull (Academic, New York, 1963), p. 44.
42. This equation is identical to Eq. (12) of J. Umeda, J. Phys. Soc. Japan 19, 2052 (1964), except for a change in sign of the coefficient of $\cos 2\theta$ owing to the difference in our definition of the angle θ .
43. C. Herring and E. Vogt, Phys. Rev. 101, 944 (1955).
44. A. C. Beer, Solid State Physics - Supplement 4, edited by F. Seitz and D. Turnbull (Academic, New York, 1963), pp. 229-231.
45. A. H. Wilson, Theory of Metals (Cambridge U. P., Cambridge, England, 1953), 2nd ed., p. 240.
46. R. S. Allgaier, Phys. Rev. 119, 554 (1960).
47. C. Herring, J. Appl. Phys. 31, 1939 (1960).
48. R. T. Bate, J. C. Bell, and A. C. Beer, J. Appl. Phys. 32, 806 (1960).
49. C. Herring, Bell System Tech. J. 34, 237 (1955), Appendix A.
50. R. A. Laff and H. Y. Fan, Phys. Rev. 112, 317 (1958).
51. G. L. Pearson and C. Herring, Physica 20, 975 (1954).
52. R. M. Broudy and J. D. Venables, Phys. Rev. 105, 1757 (1957).
53. R. L. Weiher and B. G. Dick, Jr., J. Appl. Phys. 35, 3511 (1964).
54. H. P. R. Frederikse, W. R. Hosler, and W. R. Thurber, Phys. Rev. 143, 648 (1966).

X. ACKNOWLEDGMENTS

The author wishes to thank Dr. G. C. Danielson for guiding this research. The author also wishes to thank Mr. P. H. Sidles and Mr. H. R. Shanks for several helpful discussions and Mr. O. M. Sevde and Mr. P. A. Millis for technical assistance. The mass spectrographic analysis was carried out by Mr. R. J. Conzemius of Professor H. J. Sevc's physical chemistry group in the Ames Laboratory.

XI. APPENDIX

Fig. 10. Block diagram of the apparatus.

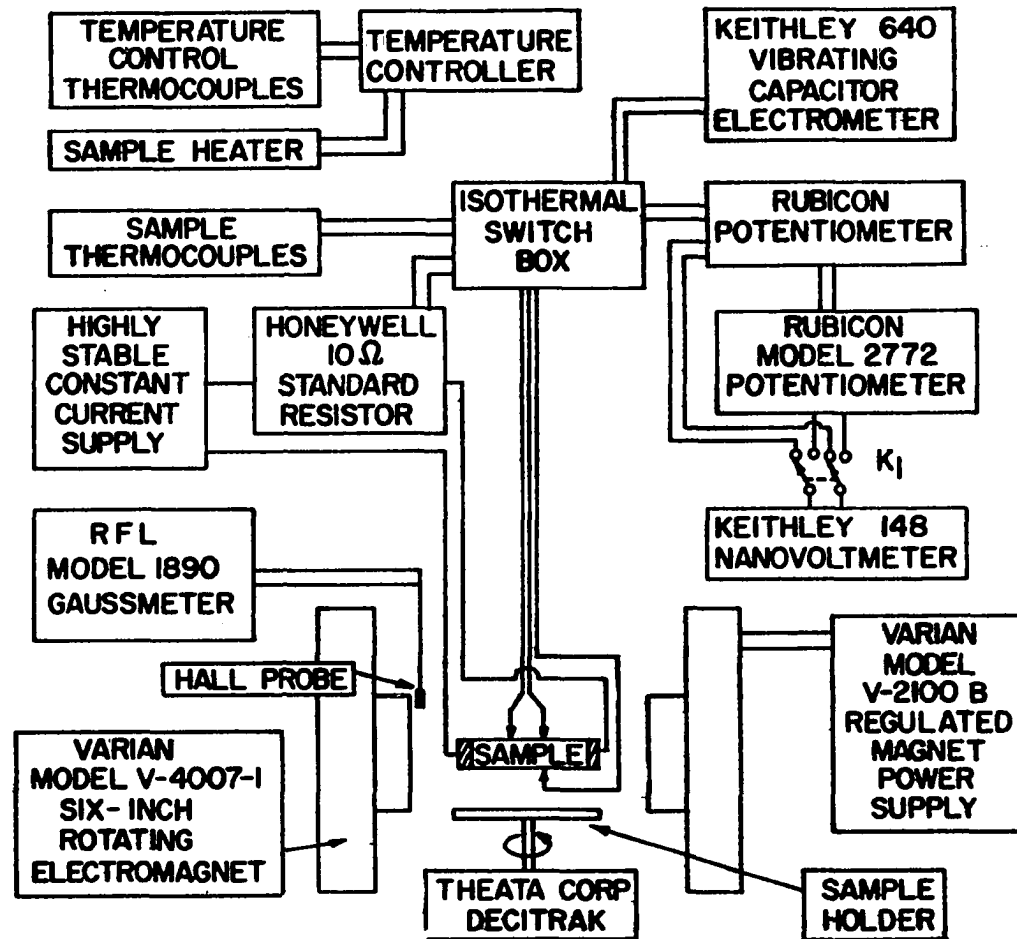


Table 4. Analysis of Mg, used in the preparation of Mg₂Ge, for impurities^a

Element	Impurity (at.ppm)
O	20.0
Cl	0.1
K	0.06
Ca	0.7
Cr	2.0
Mn	0.6
Fe	1.0
Ni	15.0
Zn	1.0

^aAnalysis was made mass spectrometrically using a Nuclides Analysis Spark Source Mass Spectrography, Nuclide Graph 2.2.

Table 5. Analysis of Mg₂Ge samples for impurities.^a

Element	Impurity (at.ppm)				
	Sample 1	Sample 4	Sample 5	Sample 6	Sample 7
Li	< 0.1	0.4	0.2	0.2	0.1
Be	< 0.03	< 0.03	< 0.03	≤ 0.03	≤ 0.03
B	2.0	< 0.2	< 0.2	10	< 0.2
O	170	40	160	280	50
Al	≤ 0.2	≤ 0.5	≤ 0.5	≤ 4.0	≤ 4.0
Si	5.0	< 5.0	< 5.0	5.0	5.0
K	1.0	0.9	1.0	3.0	3.0
Ca	170	100	200	200	200
Mn	≤ 0.7	< 0.2	< 0.2	≤ 0.2	≤ 0.2
Fe	≤ 1.0	≤ 2.0	≤ 2.0	≤ 4.0	≤ 4.0
Co	≤ 2.0	≤ 0.6	≤ 1.0	≤ 2.0	≤ 2.0
Ni	≤ 0.8	≤ 0.7	≤ 1.0	≤ 0.5	< 0.5
Cu	1.0	0.6	0.3	1.0	1.0
Zn	≤ 3.0	≤ 2.0	≤ 2.0	≤ 2.0	≤ 2.0

^a Analysis was made mass spectrometrically using a Nuclides Analysis Spark Source Mass Spectrograph, Nuclide Graph 2.2.